

Supplementary Materials for
**Sequential vacuum-evaporated perovskite solar cells with more
than 24% efficiency**

Hang Li *et al.*

Corresponding author: Chenyi Yi, yicy@mail.tsinghua.edu.cn, yicy@tsinghua.edu.cn

Sci. Adv. **8**, eabo7422 (2022)
DOI: 10.1126/sciadv.abo7422

The PDF file includes:

Figs. S1 to S32
Legends for movies S1 and S2

Other Supplementary Material for this manuscript includes the following:

Movies S1 and S2

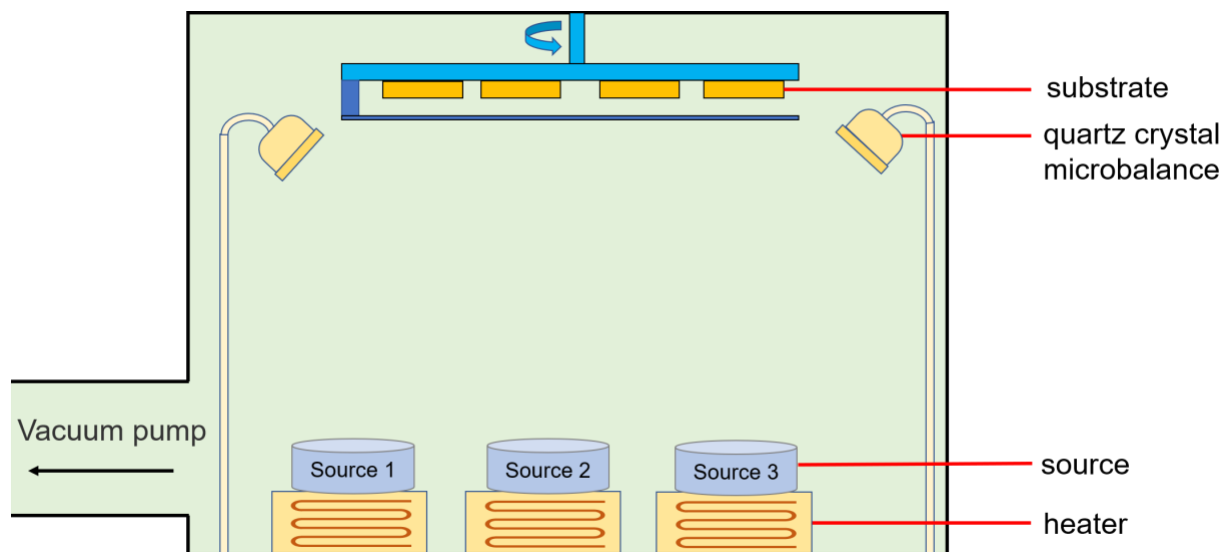


Fig. S1. Schematic illustration of vacuum chambers for the evaporation of lead halide film and FAI film.

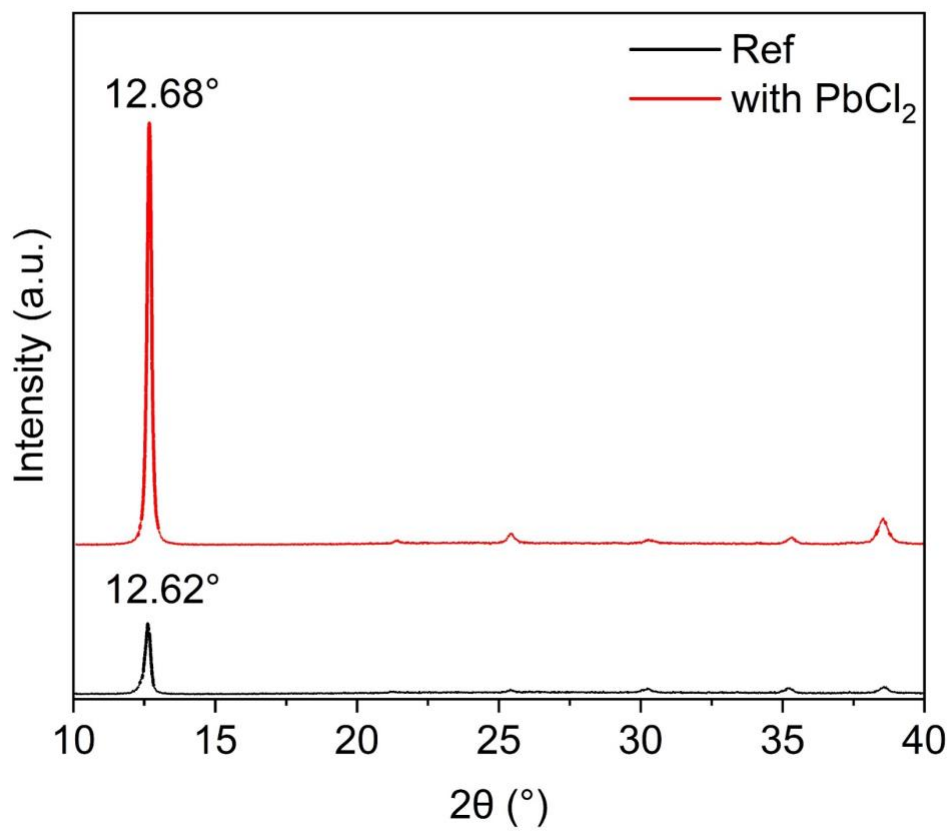


Fig. S2. XRD patterns of $\text{Cs}_{0.05}\text{PbI}_{2.05-x}\text{Cl}_x$ film and the $\text{Cs}_{0.05}\text{PbI}_{2.05}$ film.

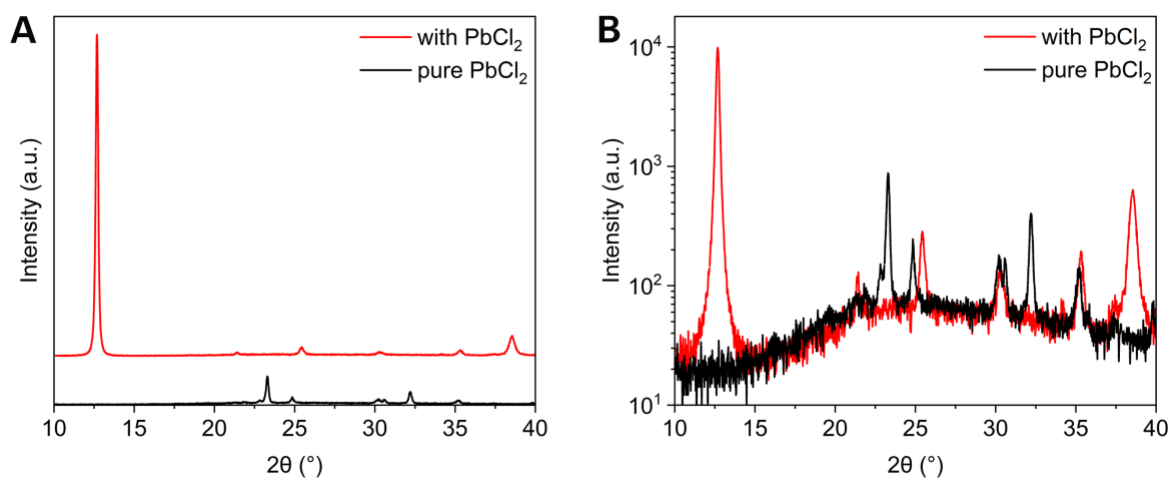


Fig. S3. XRD patterns of $\text{Cs}_{0.05}\text{PbI}_{2.05-x}\text{Cl}_x$ film and pure PbCl_2 film with (A) linear Y scale and (B) log Y scale.

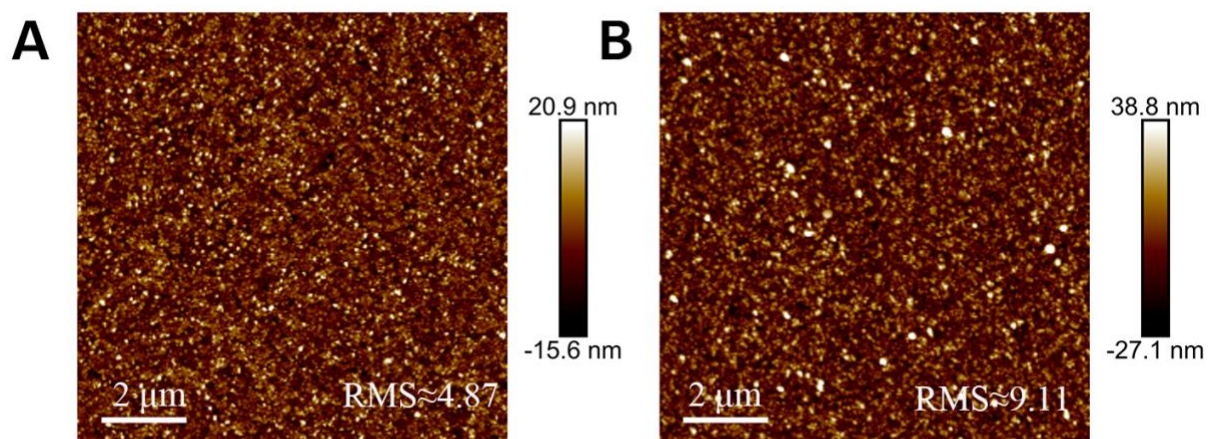


Fig. S4. AFM images of (A) $\text{Cs}_{0.05}\text{PbI}_{2.05-x}\text{Cl}_x$ film and (B) $\text{Cs}_{0.05}\text{PbI}_{2.05}$ film.

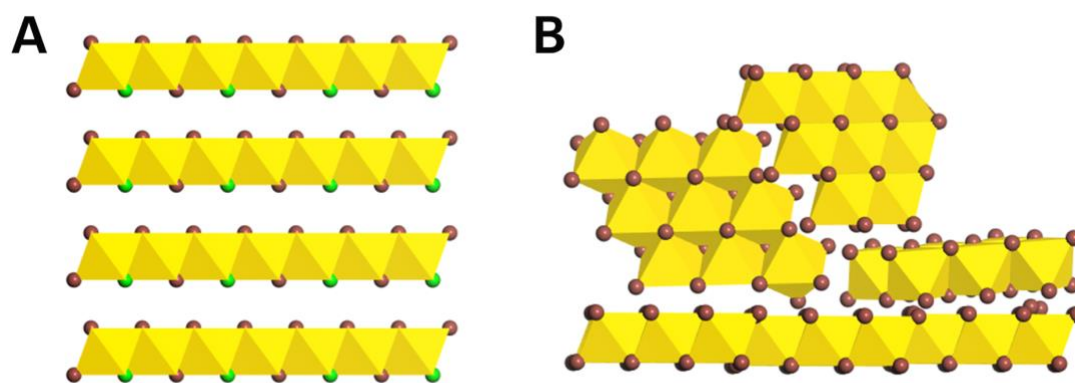


Fig. S5. Schematic illustrations of the lead halide skeleton orientation.

Lead halide skeleton orientation of (A) Cs_{0.05}PbI_{2.05-x}Cl_x film (B) Cs_{0.05}PbI_{2.05} film. The green atom represents chlorine and the brown for the iodine.

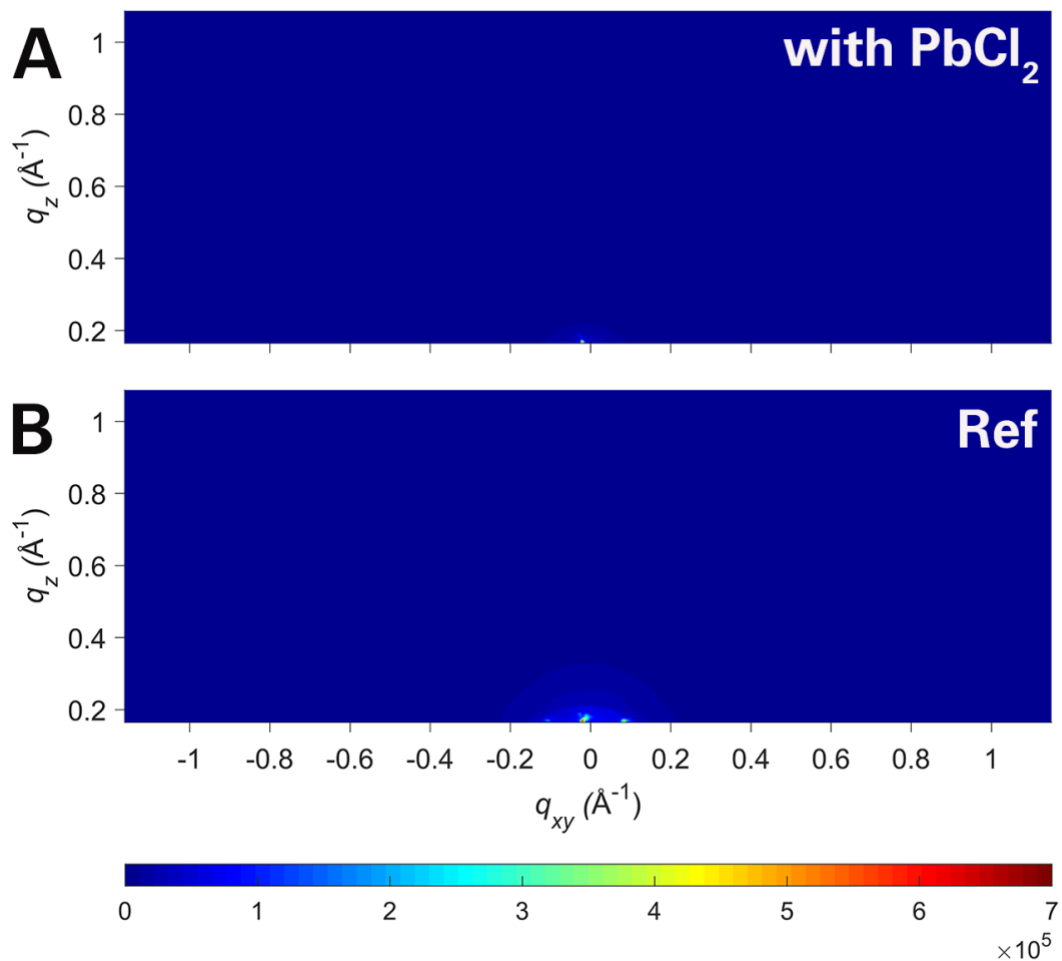


Fig. S6. GIWAXS patterns of (A) the Cl-alloy mediated film and (B) the Ref film at an incident angle of 0.1° before annealing.

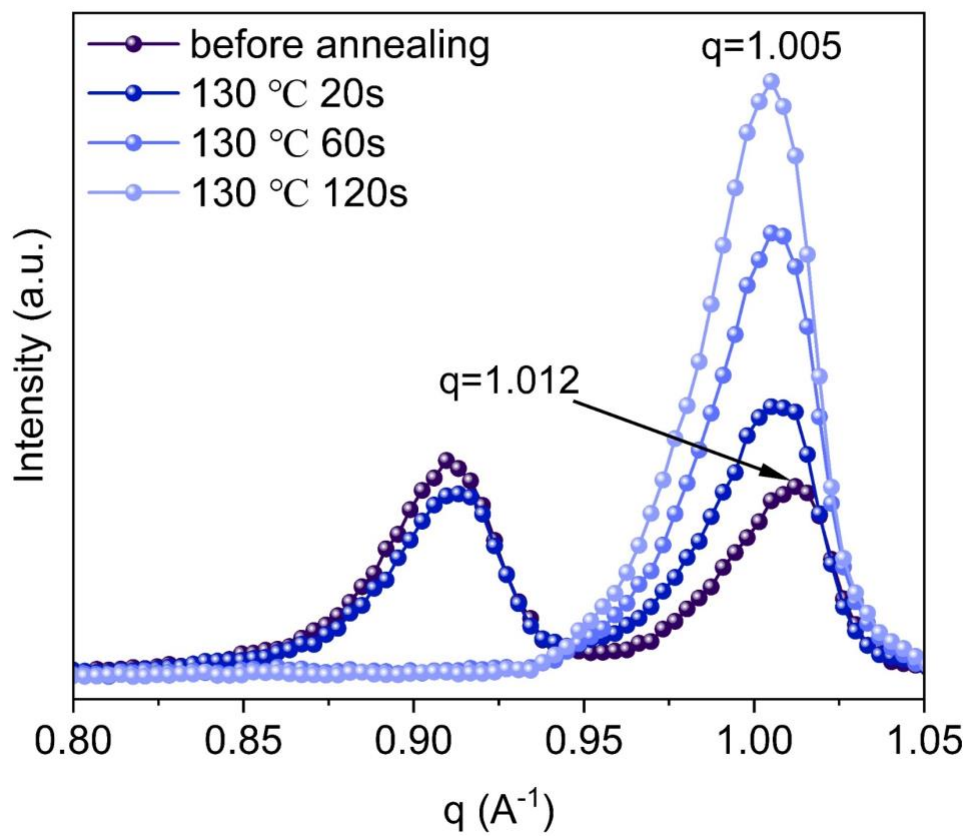


Fig. S7. In-situ GIXRD characterization of Cl-alloy mediated perovskite film with different annealing time at 130°C.

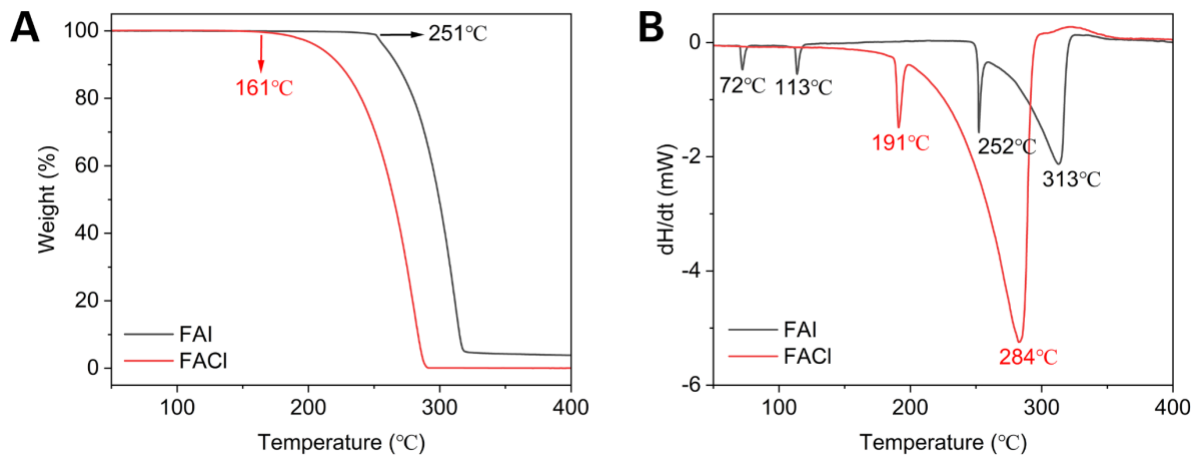


Fig. S8. TGA (A) and DSC (B) results of FAI and FAcI powders.

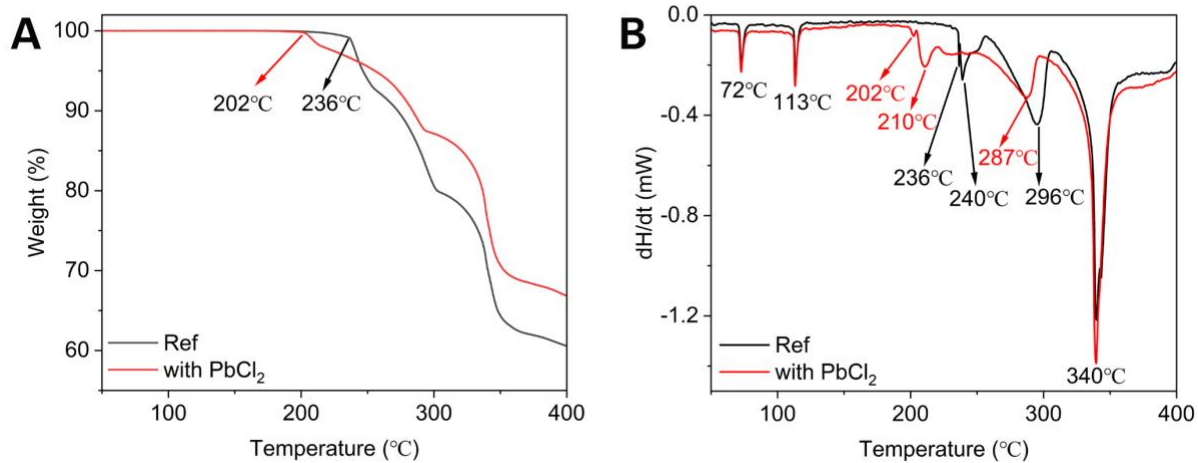


Fig. S9. TGA (A) and DSC (B) results of the powders with the composition of the Cl-alloy mediated perovskite film and the Ref film.

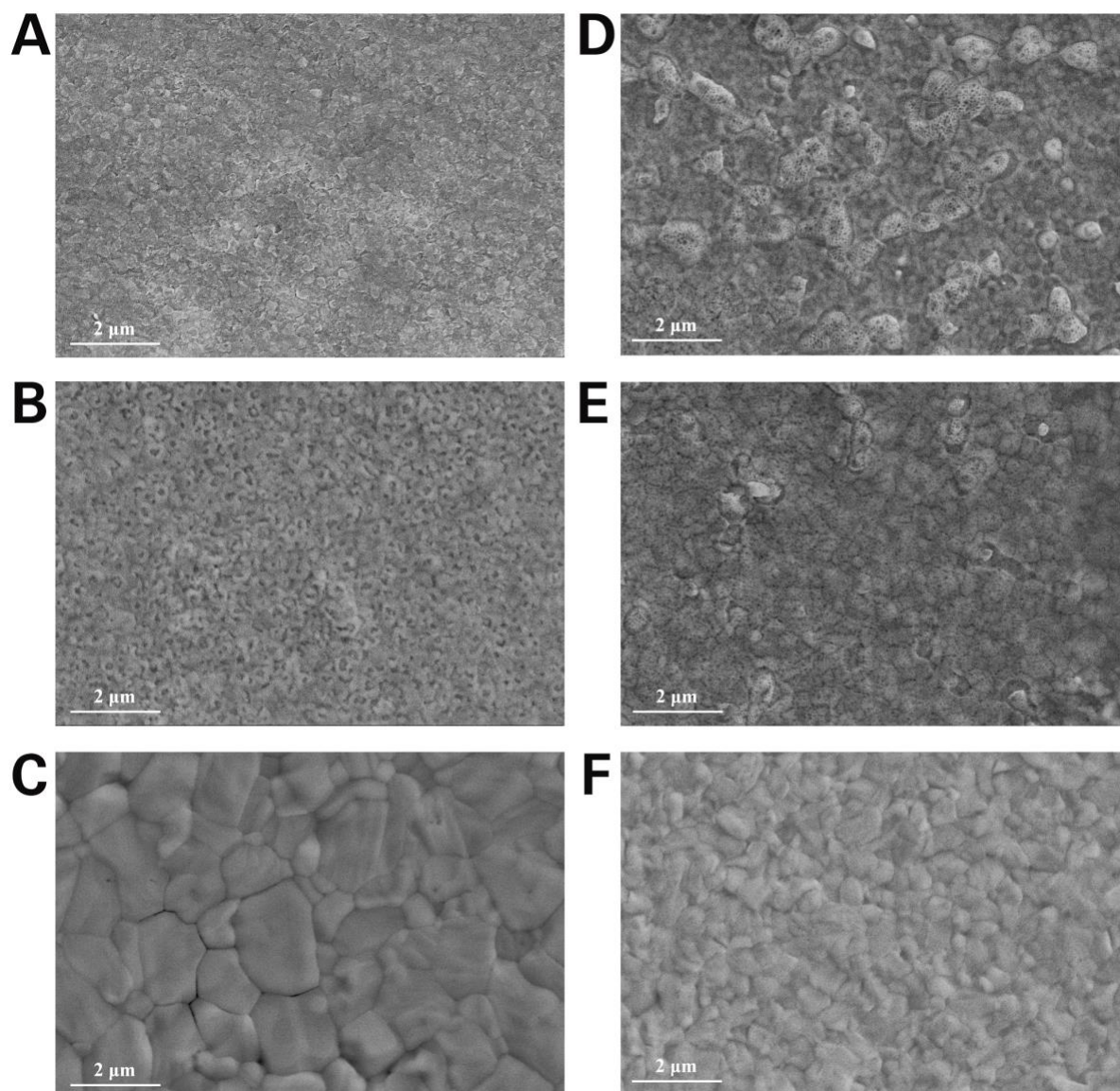


Fig. S10. Morphology evolution of perovskite film surface during the annealing process.

(A to C) SEM images of the C1-alloy mediated film at different annealing temperature with different annealing time in ambient air. (A) without annealing (B) 130°C 30 s (C) 170°C 1 min. (D to F) SEM images of the Ref film at different annealing temperature with different annealing time in ambient air. (D) without annealing (E) 130°C 30 s (F) 170°C 1 min.

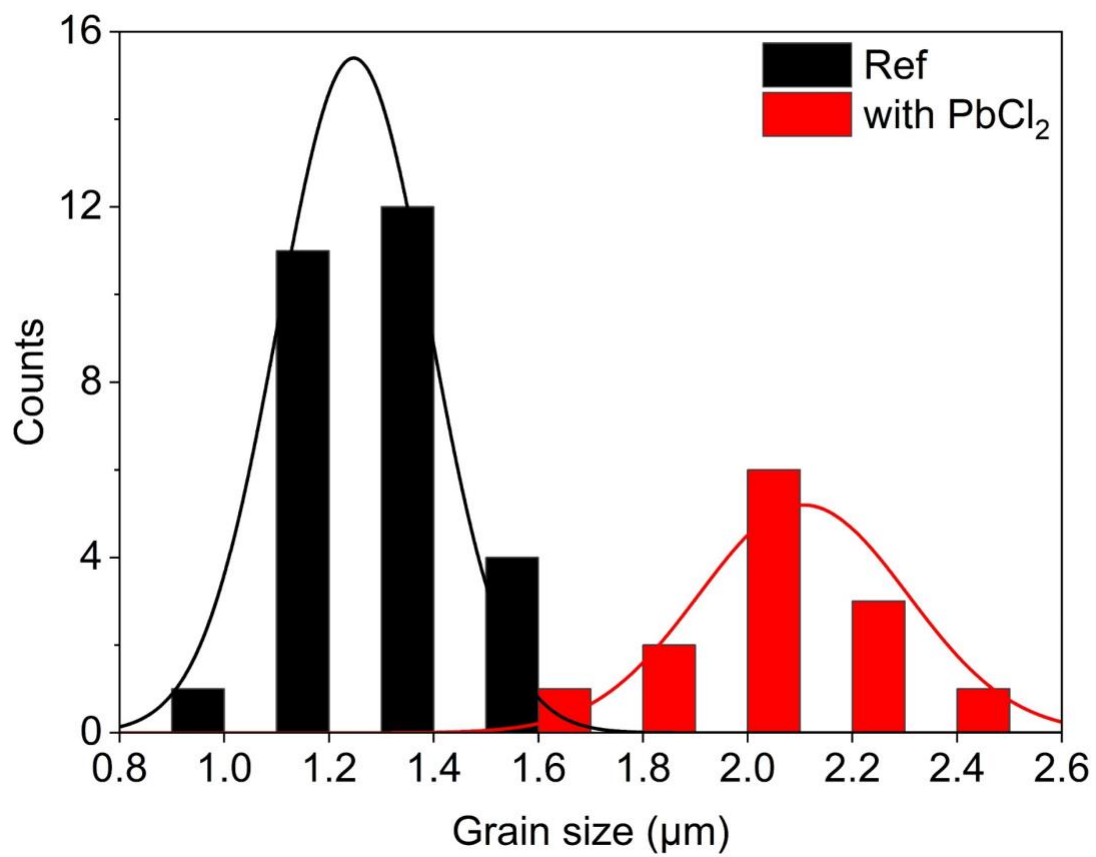


Fig. S11. Grain size statistics of the Cl-alloy mediated perovskite film and the Ref film.

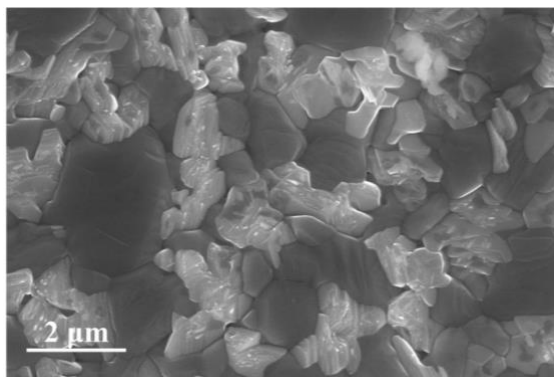


Fig. S12. Top-view SEM images of the Cl-alloy mediated perovskite film.
The SEM detector is InlensDuo.

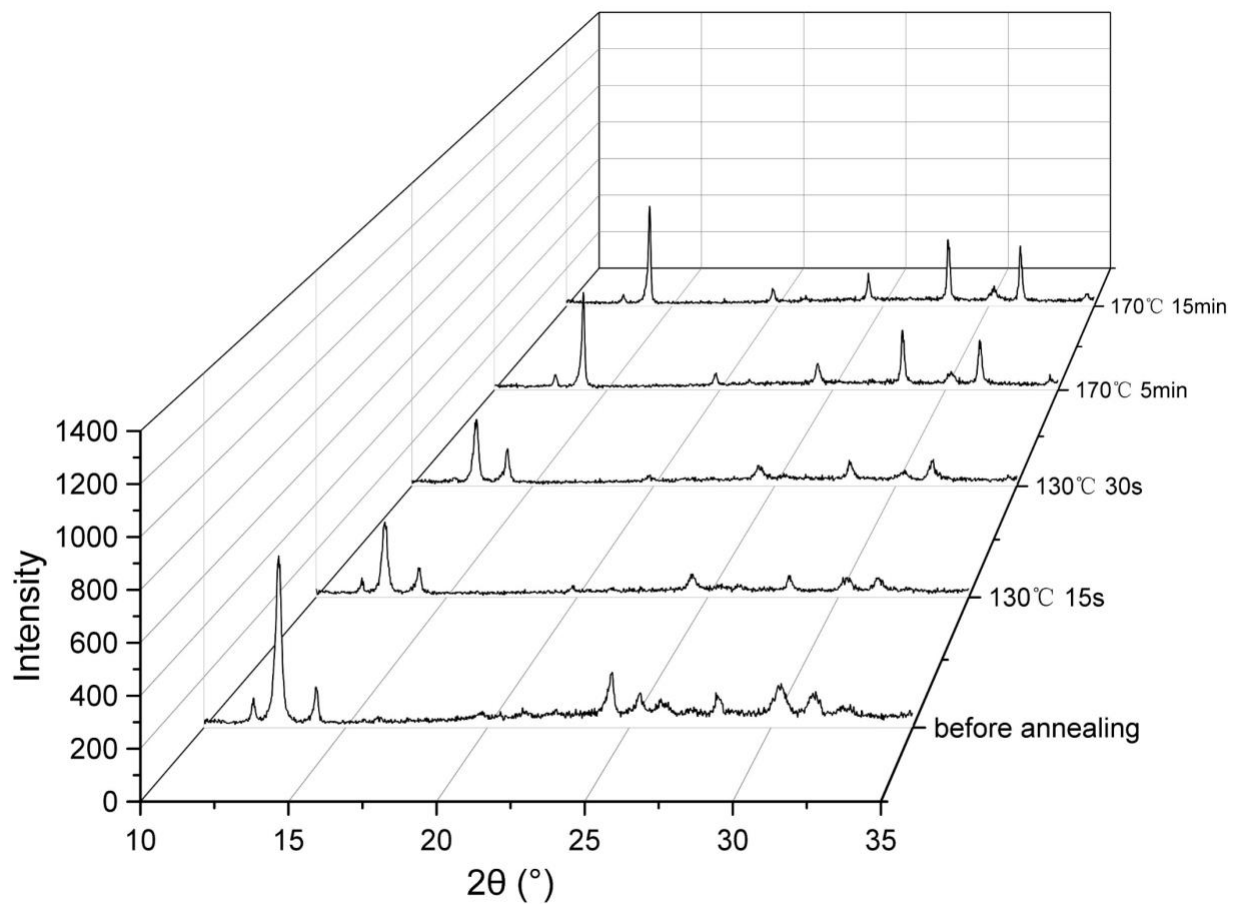


Fig. S13. XRD patterns of the Ref perovskite films with different annealing temperature and time.

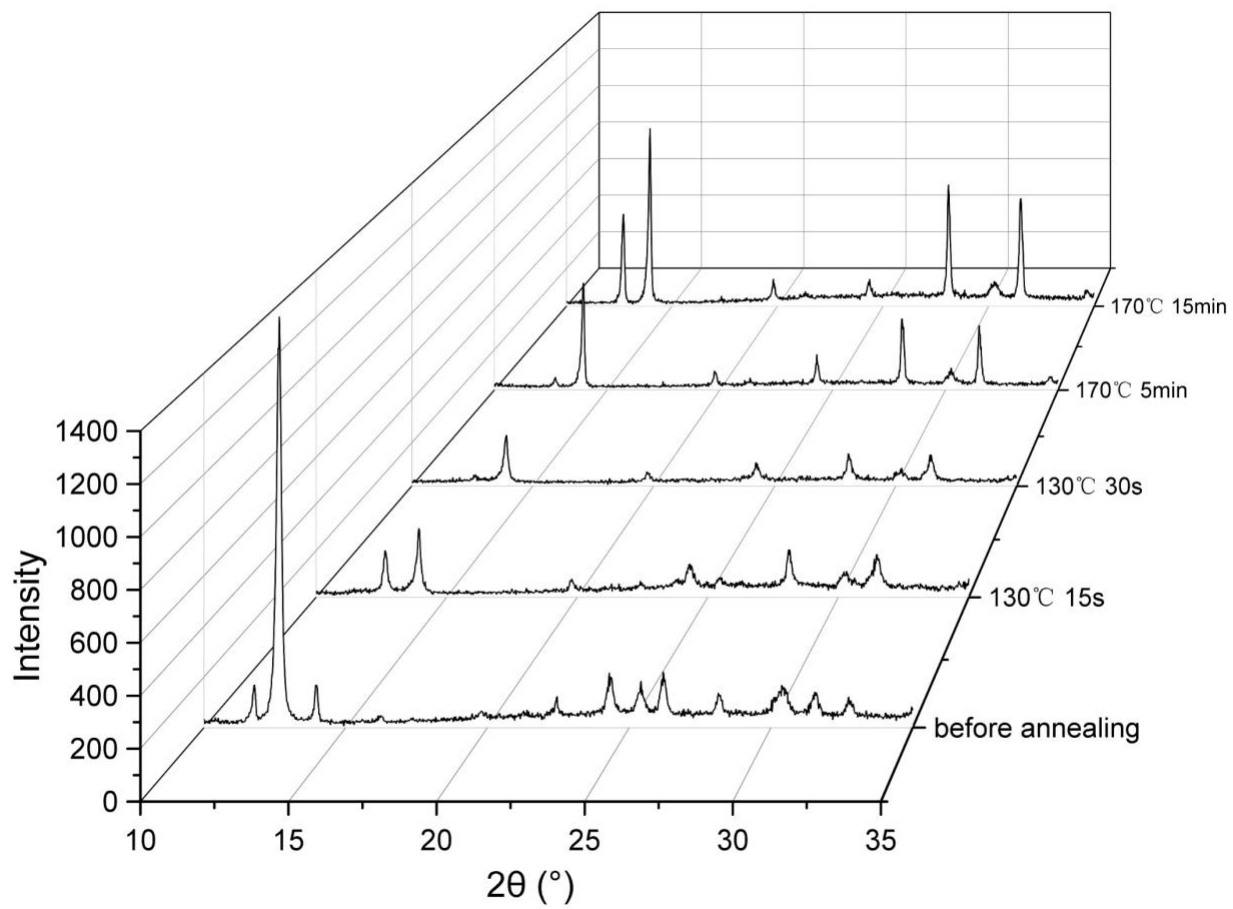


Fig. S14. XRD patterns of the CI-alloy mediated perovskite films with different annealing temperature and time.

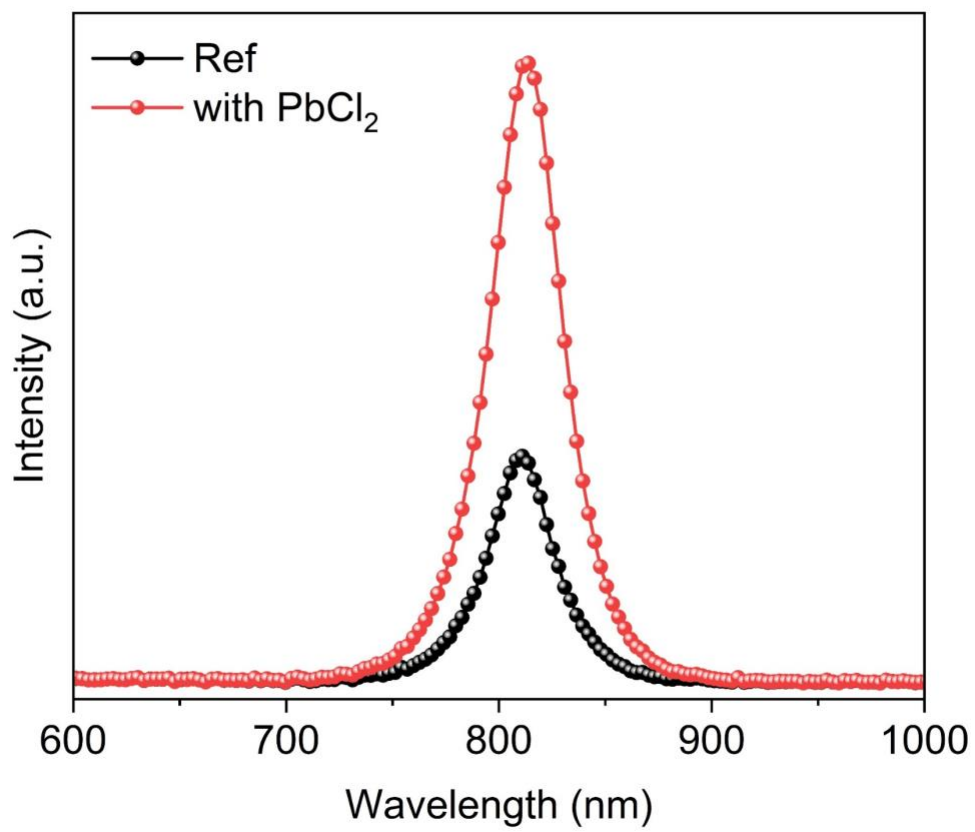


Fig. S15. EL spectra of the Ref PSC and Cl-alloy-mediated PSC measured under 1.5 V bias voltage.

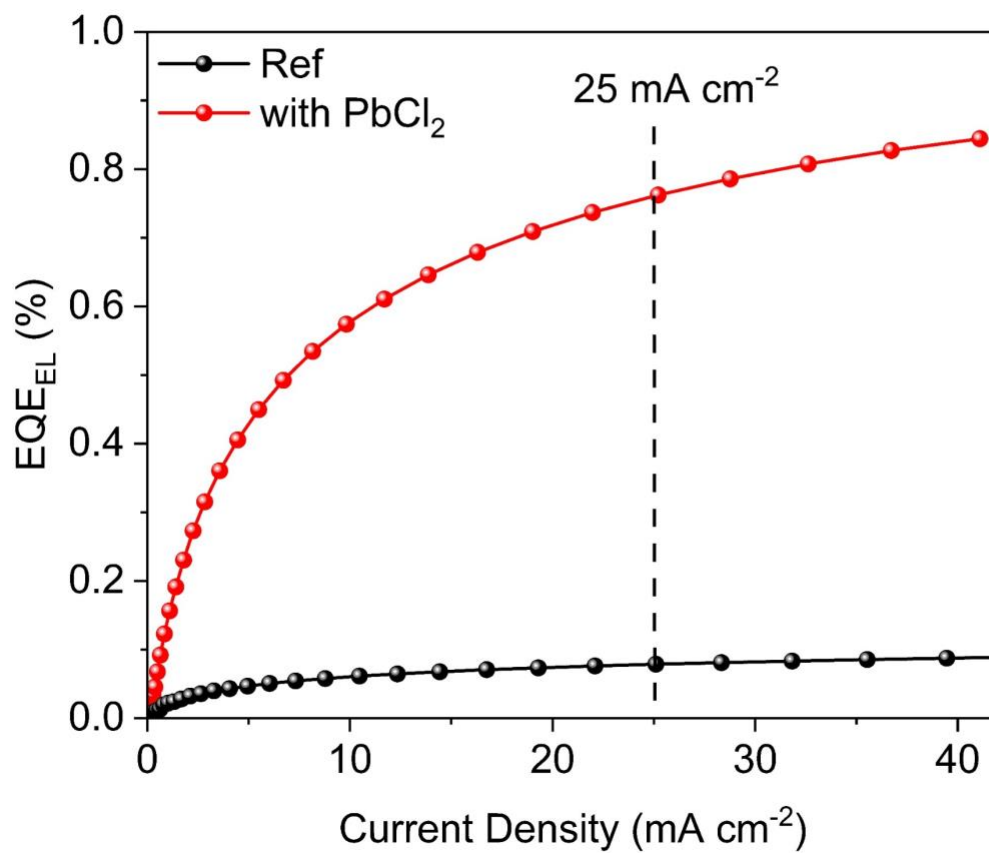


Fig. S16. EQE curves of EL on the Cl-alloy mediated PSC and the Ref PSC under different current densities.

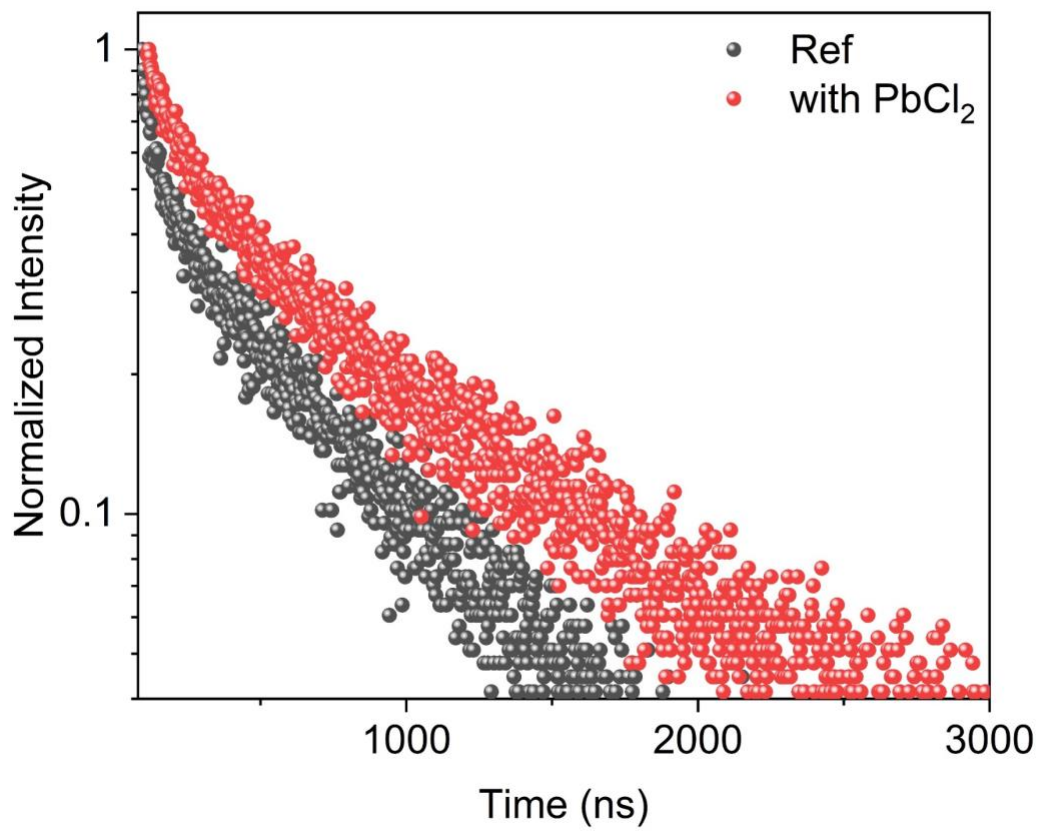


Fig. S17. TRPL spectroscopy of the Cl-alloy mediated perovskite film and the Ref film.

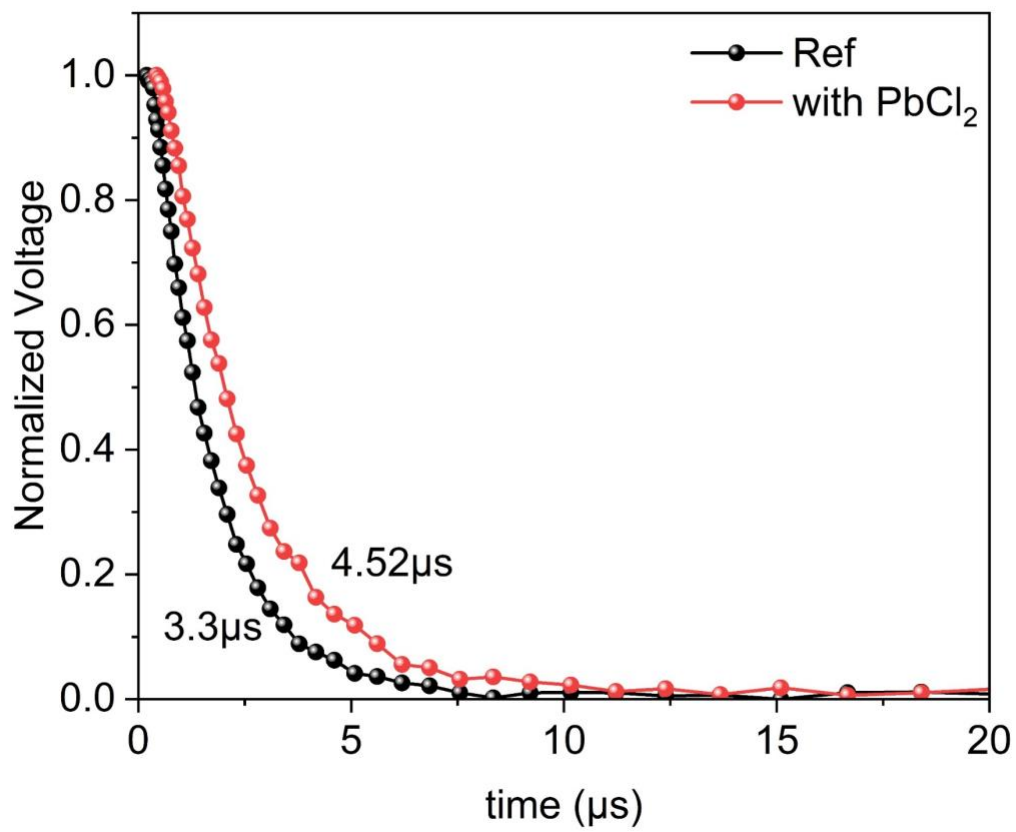


Fig. S18. Normalized TPV curves of Ref and Cl-alloy mediated PSCs.

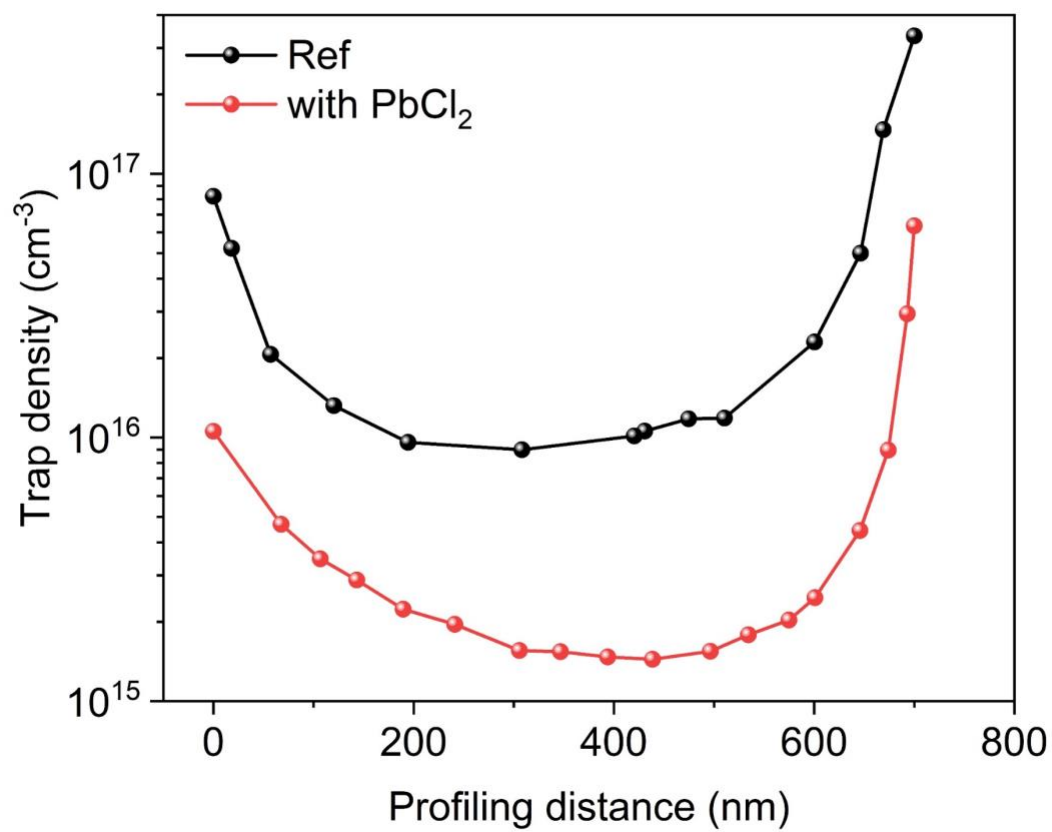


Fig. S19. Dependence of the trap density on the profiling distance for the Ref and Cl-alloy mediated PSCs measured at an AC frequency of 10 kHz.

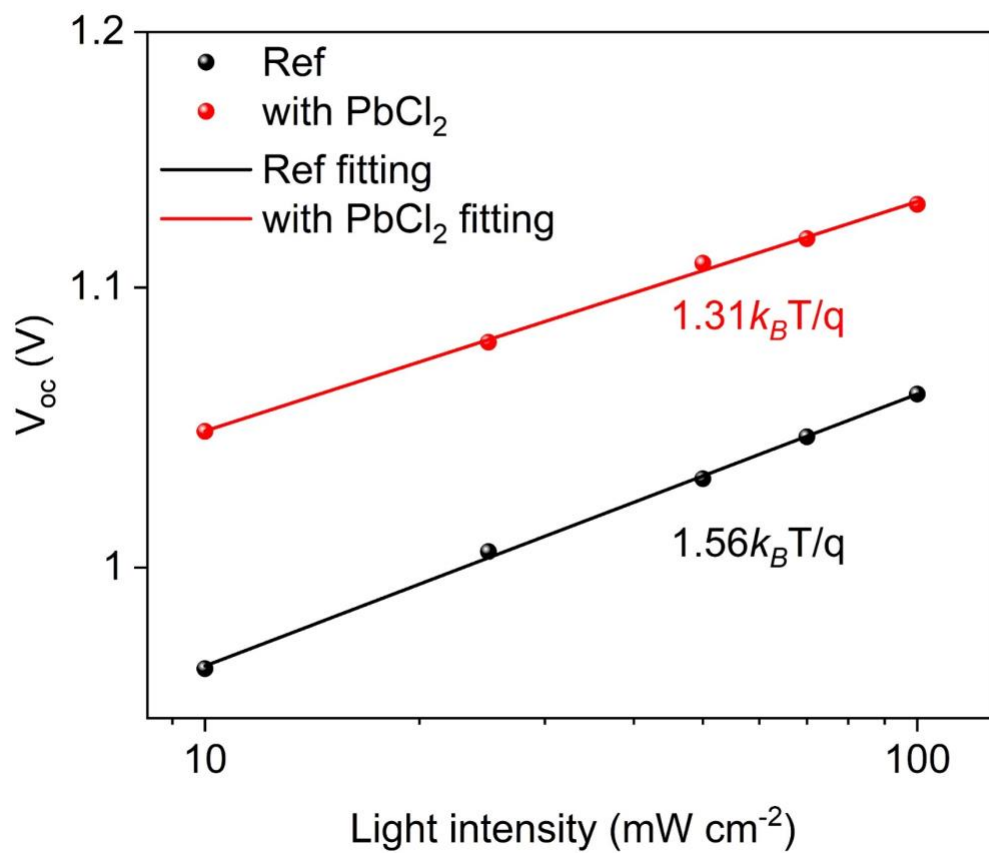


Fig. S20. Light intensity dependence of the V_{oc} of PSCs.

k_B is the Boltzmann constant and T is the absolute temperature.

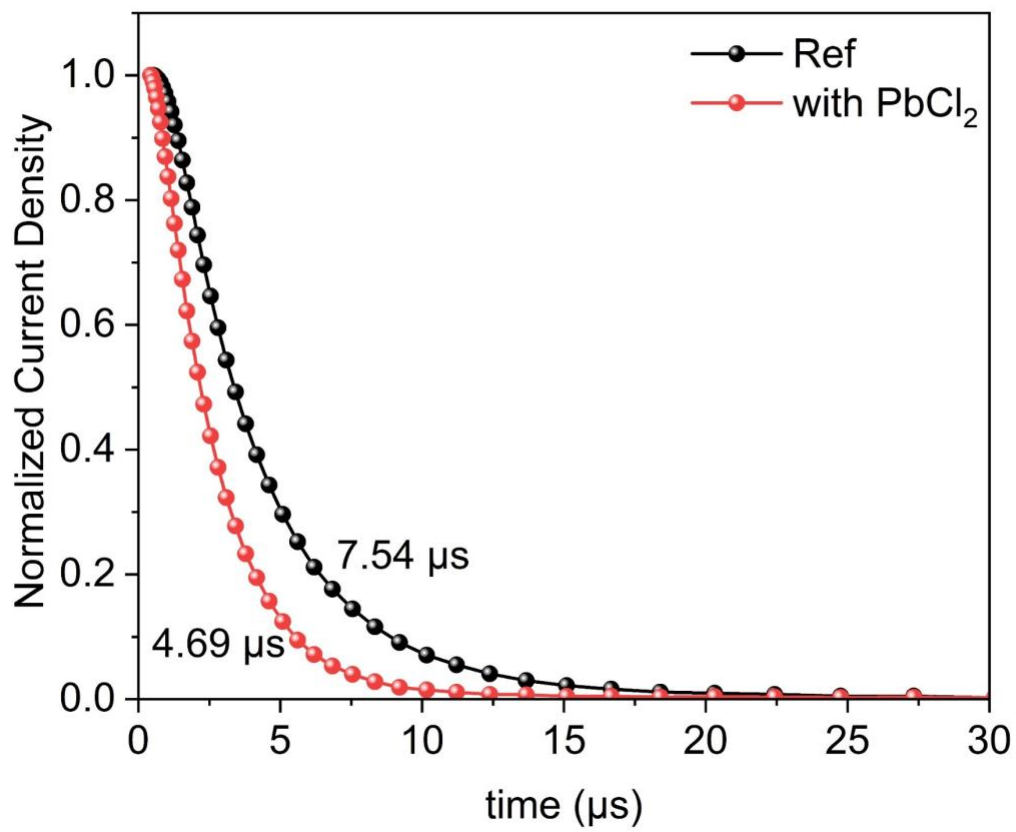


Fig. S21. Normalized TPC curves of the Ref and Cl-alloy mediated PSCs.

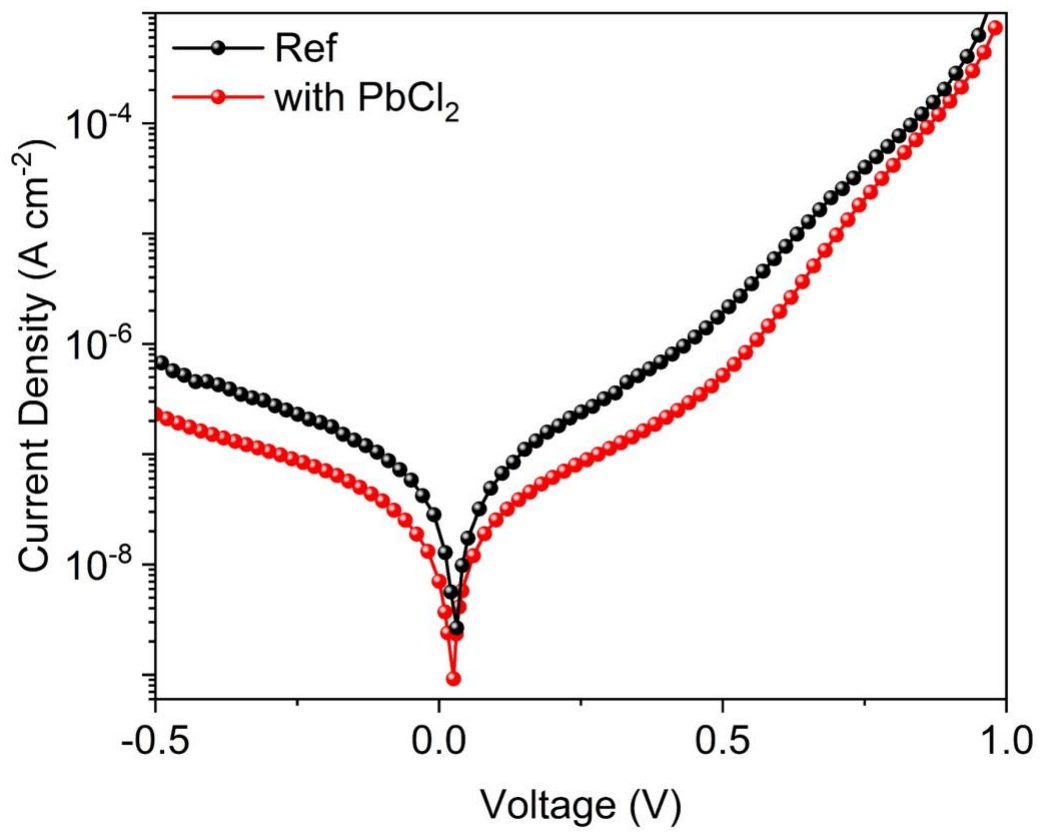


Fig. S22. Dark J - V curves of the Ref and Cl-alloy mediated PSCs.

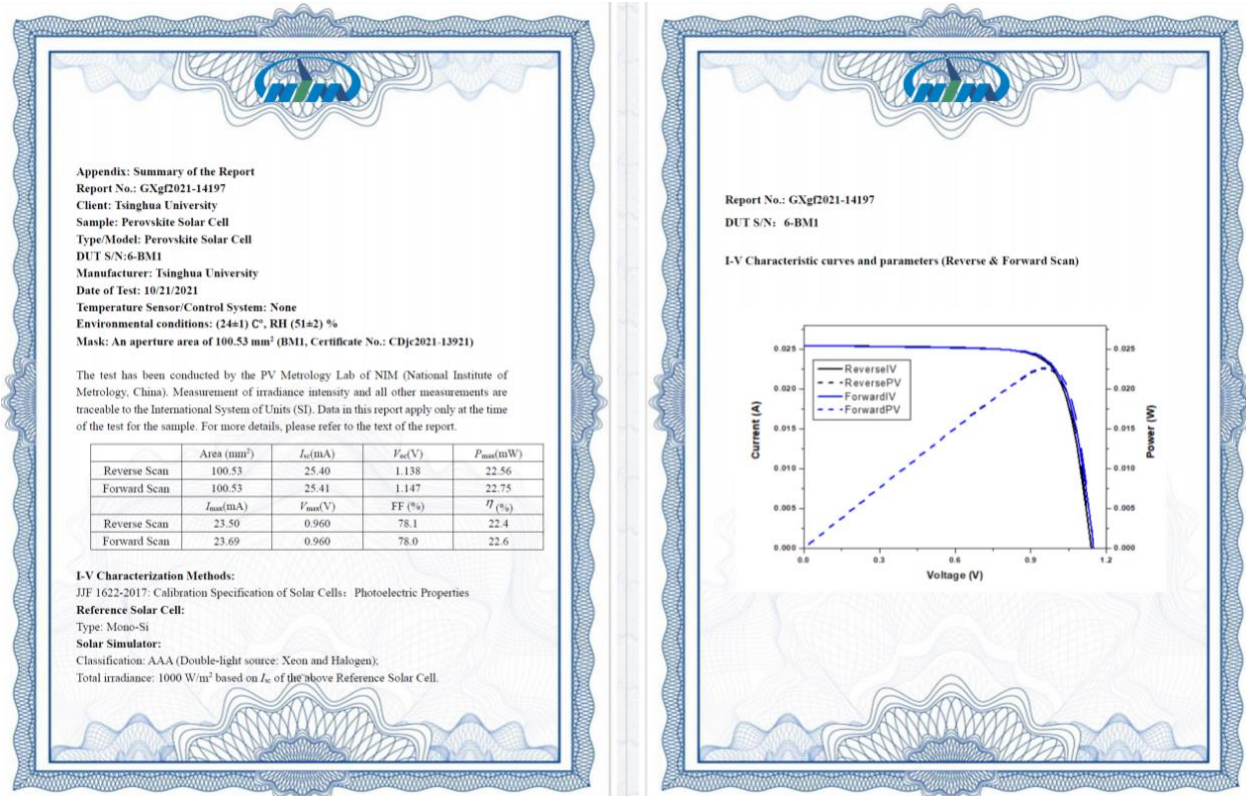


Fig. S23. Certificated results from PV Metrology Lab of NIM (National Institute of Metrology, China).

The aperture area of 1.0053 cm² was defined by a metal mask.

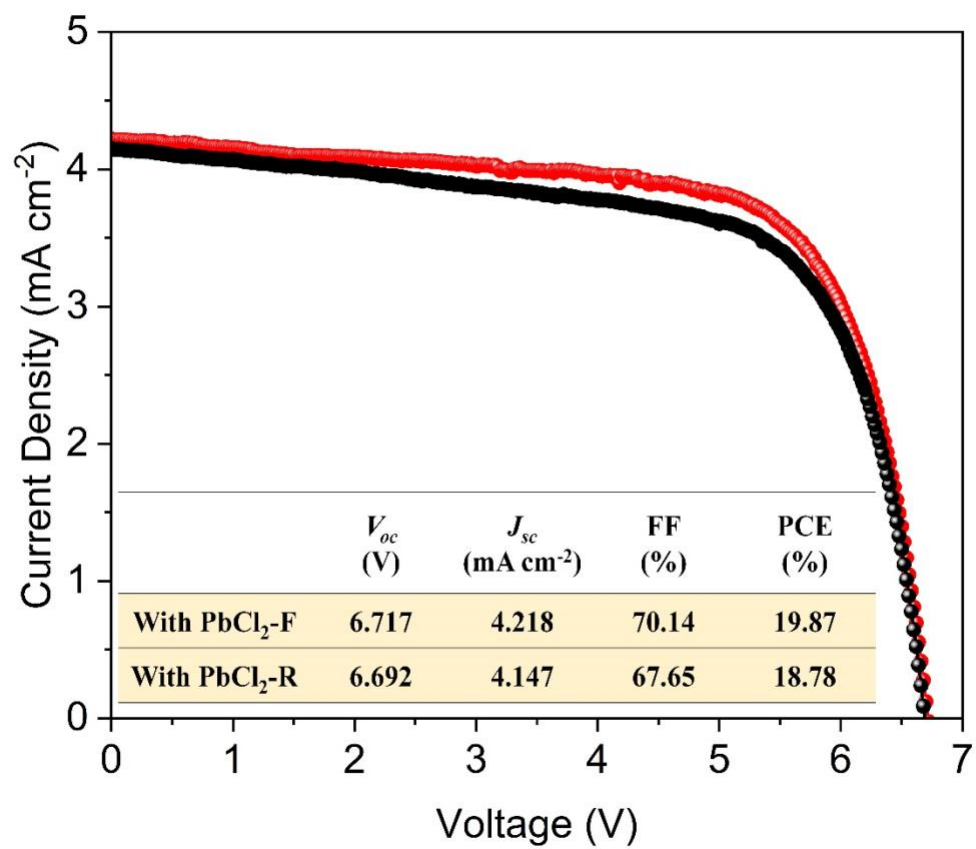


Fig. S24. *J-V* curve and corresponding parameters of the vacuum evaporated PSC module (14.4 cm² aperture area).

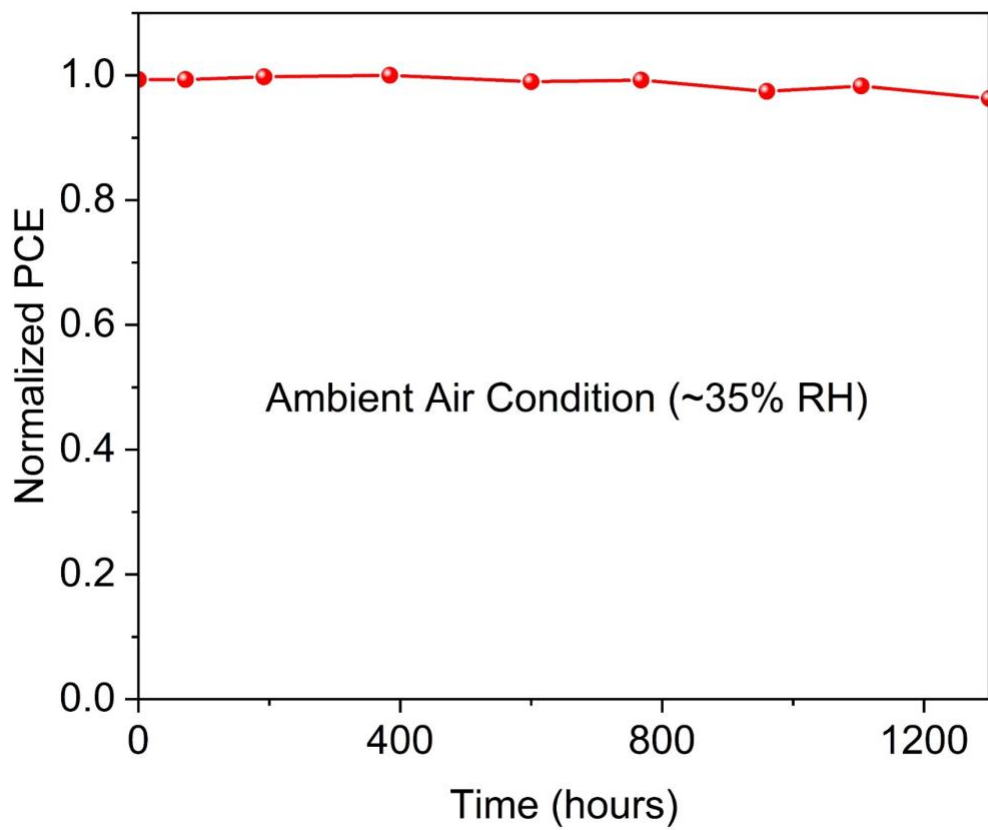


Fig. S25. The long-term environmental stability of unencapsulated Cl-alloy mediated PSCs exposed to an atmospheric environment of 35% humidity in the dark.

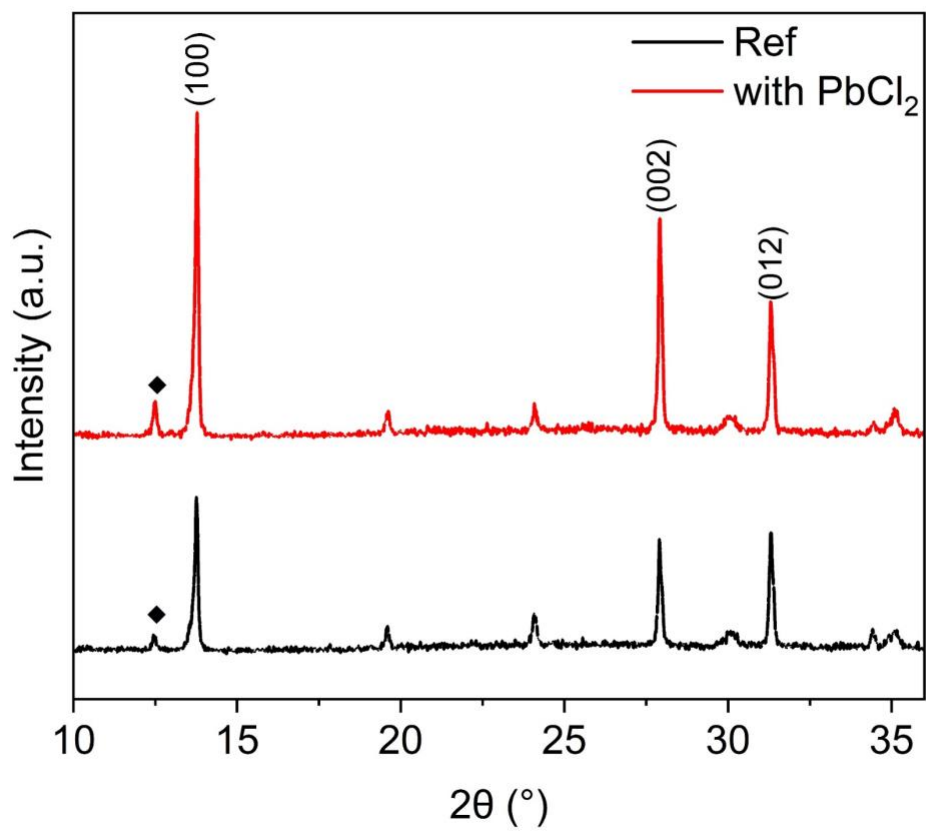


Fig. S26. XRD patterns of Cl-alloy mediated perovskite film and the Ref film after annealing at 170°C for 15 min in ambient air.

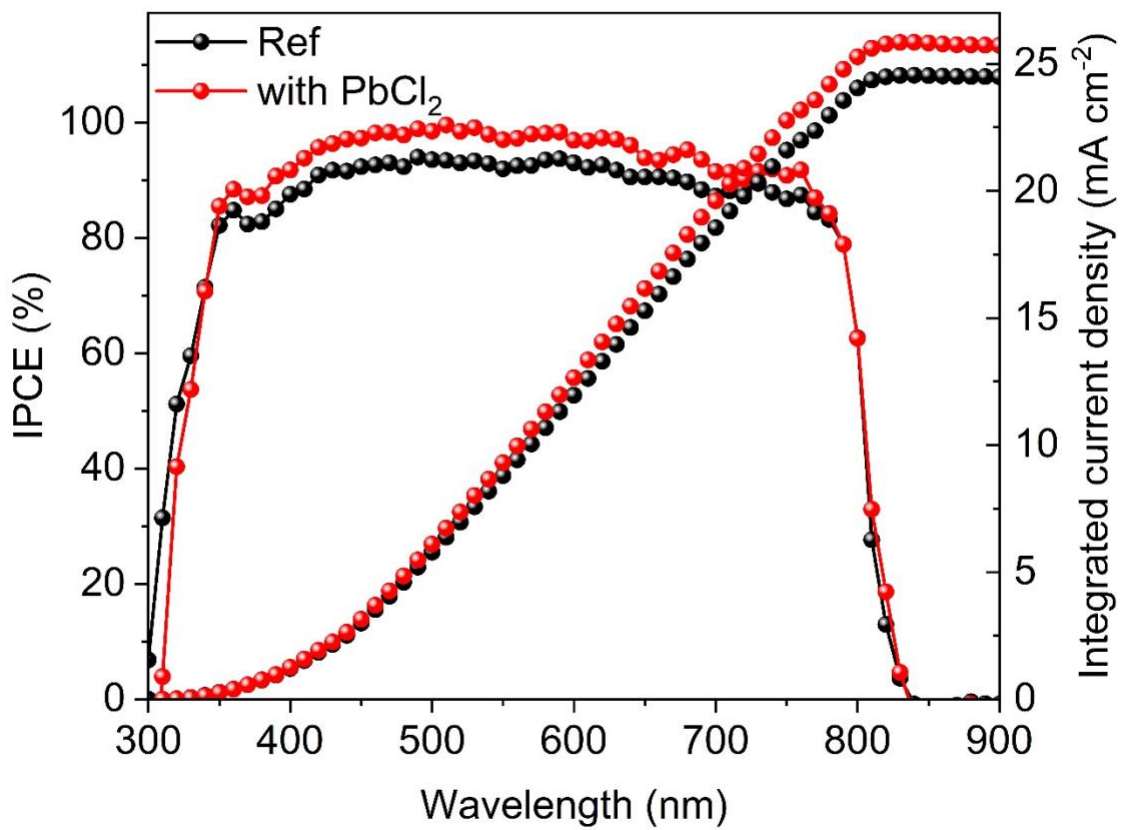


Fig. S27. IPCE curve of the Cl-alloy mediated PSC and the Ref PSC over 300 to 900 nm wavelengths and integrated J_{sc} over the AM1.5G standard spectrum.

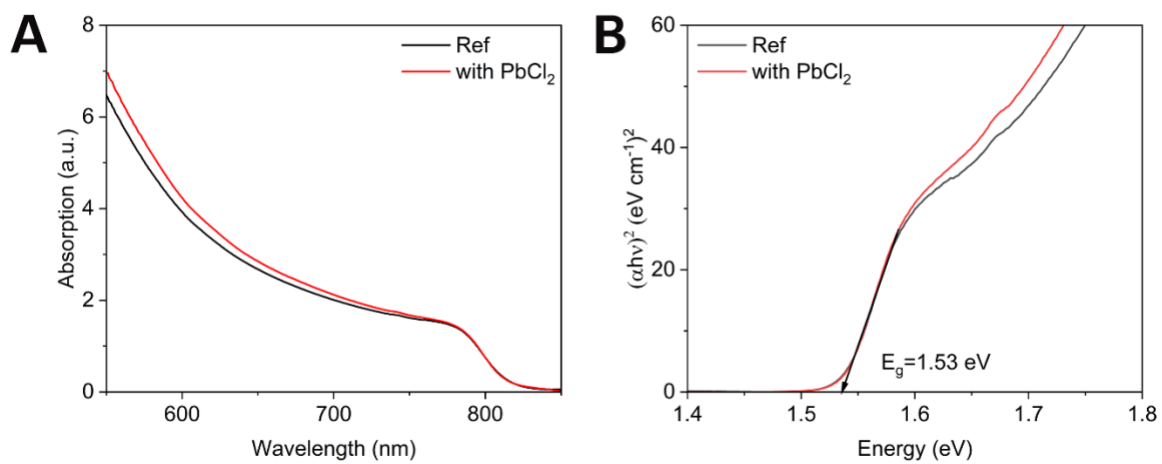


Fig. S28. (A) UV-vis spectra and (B) Tauc plot of the Ref perovskite film and Cl-alloy mediated perovskite film.

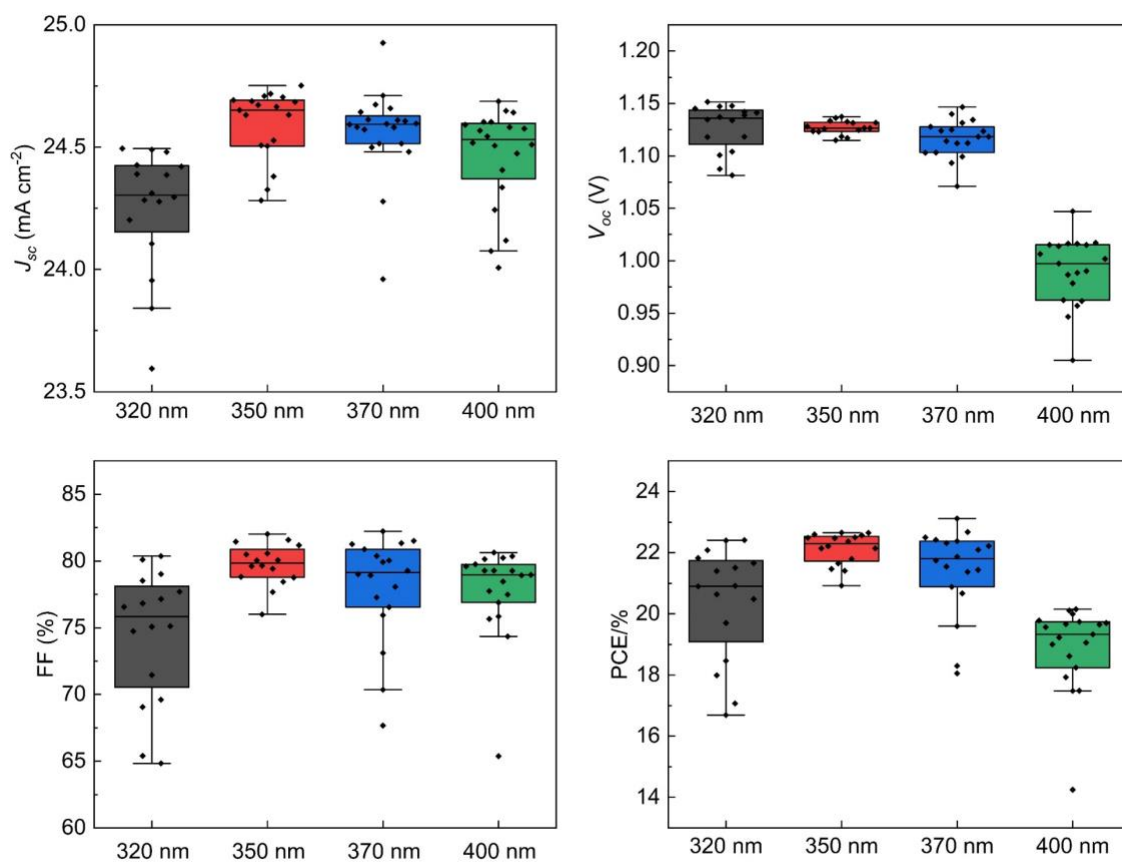


Fig. S29. Statistics of photovoltaic parameters (J_{sc} , V_{oc} , FF, PCE, respectively) of Cl-alloy mediated PSCs with different FAI thickness.

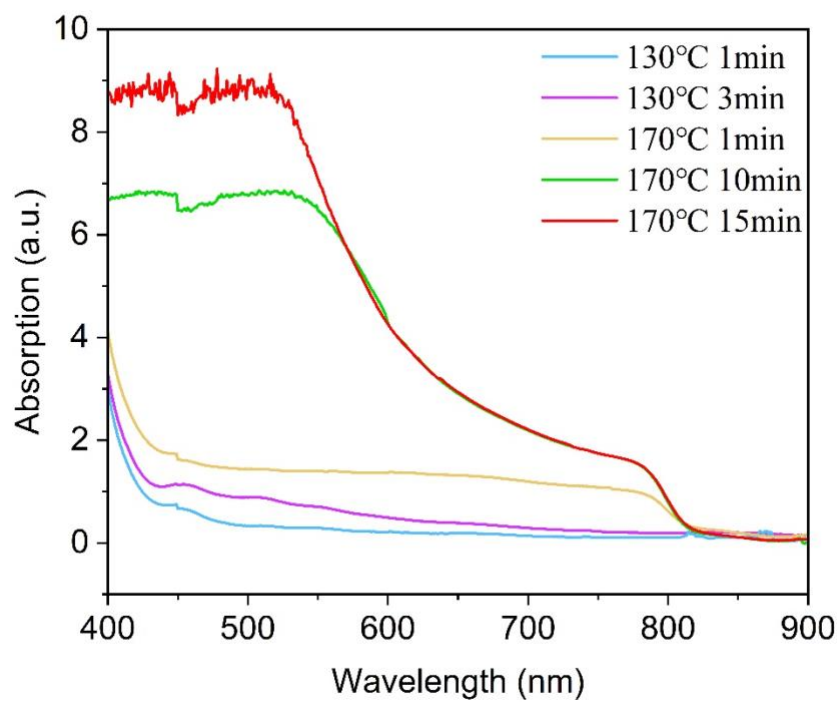


Fig. S30. UV-vis spectra of the Cl-alloy mediated perovskite film with different annealing temperature and time.

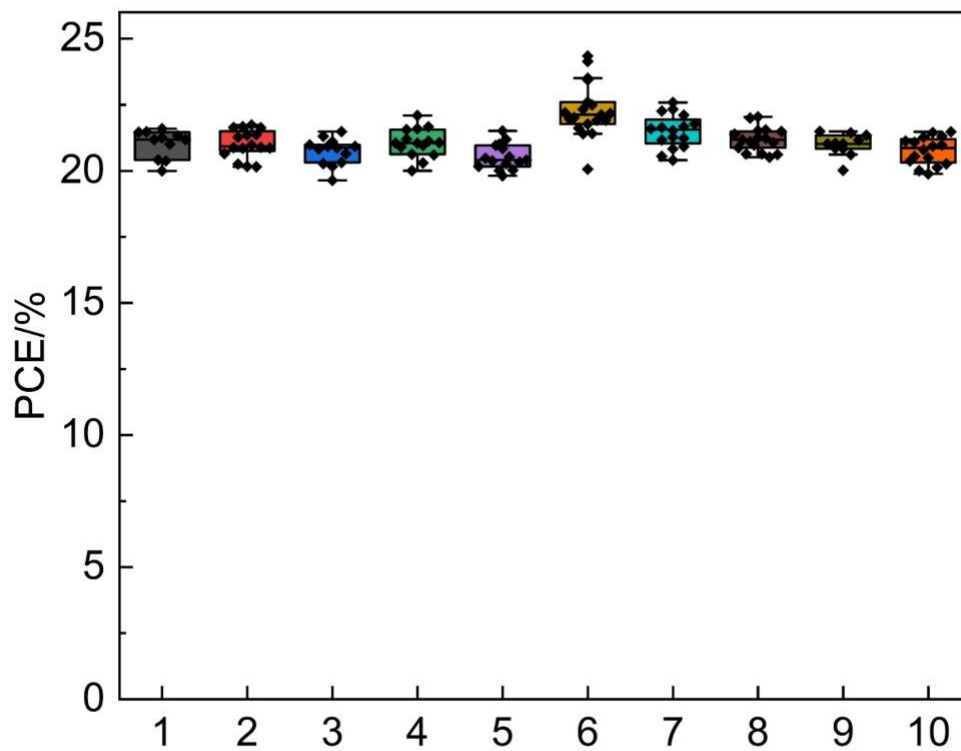


Fig. S31. PCE results from $J-V$ measurement of 10 batches of CI-alloyed PSCs.

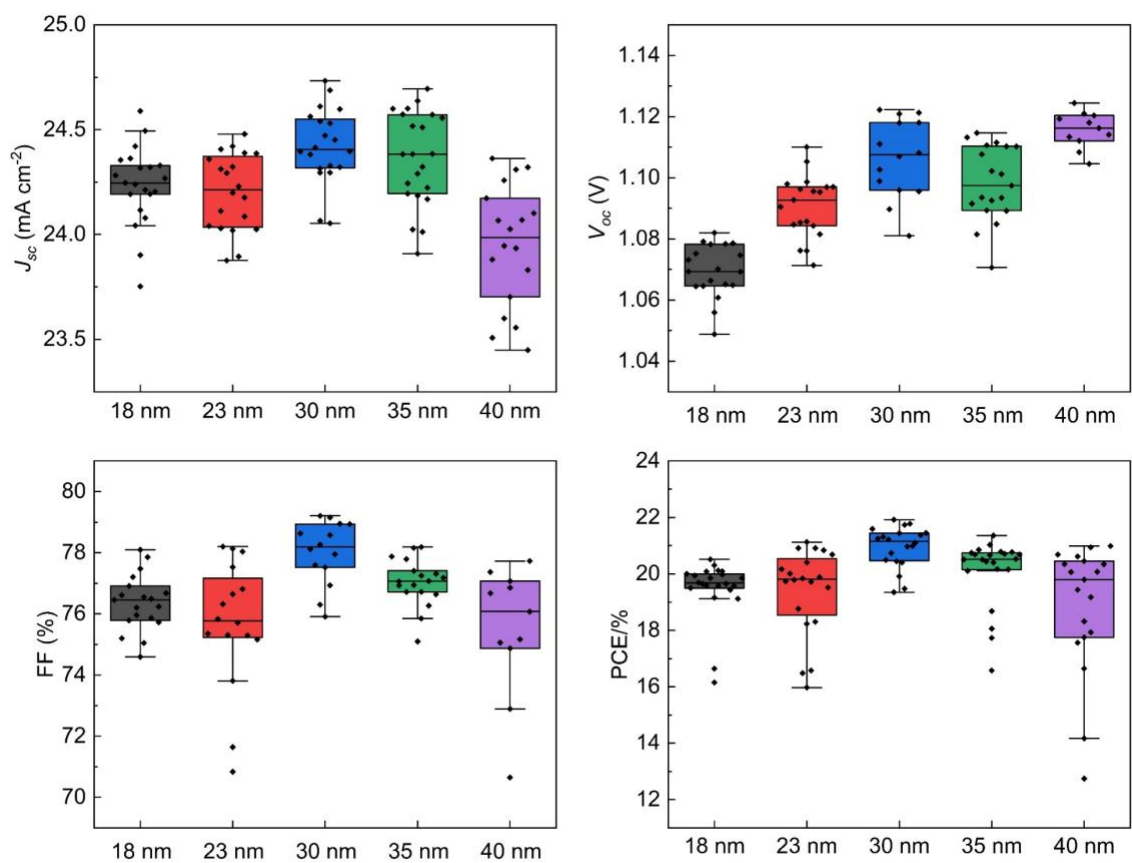


Fig. S32. Statistics of photovoltaic parameters (J_{sc} , V_{oc} , FF, PCE, respectively) of Cl-alloy mediated PSCs with different PbCl₂ thickness.

Movie S1.

in-Operando GIWAXS of the PbCl₂-alloyed perovskite films annealed at 130°C for 10 min and 170°C for 15 min.

Movie S2.

in-Operando GIWAXS of Ref perovskite films annealed at 130°C for 10 min and 170°C for 15 min.